Vol 15 No 3, March 2006
1009-1963/2006/15(03)/0575-05
Chinese Physics
© 2006 Chin. Phys. Soc.
and IOP Publishing Ltd

Surface properties of diamond-like carbon films prepared by CVD and PVD methods*

Liu Dong-Ping(刘东平)[a)†], Liu Yan-Hong(刘艳红)[b)], and Chen Bao-Xiang(陈宝祥)[a)]

[a)] *Department of Mathematics and Physics, Dalian Nationality University, Dalian 116600, China*
[b)] *State Key Laboratory for Material Modification by Laser, Ion and Electron Beams, Dalian University of Technology, Dalian 116024, China*

(Received 12 August 2005; revised manuscript received 12 October 2005)

Diamond-like carbon (DLC) films have been deposited using three different techniques: (a) electron cyclotron resonance—plasma source ion implantation, (b) low-pressure dielectric barrier discharge, (c) filtered—pulsed cathodic arc discharge. The surface and mechanical properties of these films are compared using atomic force microscope-based tests. The experimental results show that hydrogenated DLC films are covered with soft surface layers enriched with hydrogen and sp^3 hybridized carbon while the soft surface layers of tetrahedral amorphous carbon (ta-C) films have graphite-like structure. The formation of soft surface layers can be associated with the surface diffusion and growth induced by the low-energy deposition process. For typical CVD methods, the atomic hydrogen in the plasmas can contribute to the formation of hydrogen and sp^3 hybridized carbon enriched surface layers. The high-energy ion implantation causes the rearrangement of atoms beneath the surface layer and leads to an increase in film density. The ta-C films can be deposited using the medium energy carbon ions in the highly-ionized plasma.

Keywords: diamond-like carbon film, film deposition, atomic force microscope
PACC: 5250D, 6855, 0779

1. Introduction

Diamond-like carbon (DLC) is a metastable form of amorphous carbon (a-C) or hydrogenated amorphous carbon (a-C:H) containing a significant fraction of sp^3 C–C bonding. The superhard hydrogen-free tetrahedral amorphous carbon film (ta-C) and hydrogenated tetrahedral DLC film (ta-C:H) contain an extremely high sp^3 bonded fraction as approaching diamond structure. DLC films may be deposited by various physical and chemical vapour deposition techniques, such as sputtering of graphite,[1] cathodic arc discharge,[2] laser vaporization,[3] plasma source ion implantation,[4] r.f. chemical vapour deposition (CVD),[5,6] electron cyclotron resonance (ECR)-CVD,[7,8] and dielectric barrier discharge (DBD).[9] The formation of an sp^3 bonded carbon is important for synthesizing DLC films. An ion implantation mode[3−5,8−10] was proposed for forming metastable amorphous films, in which sp^3 bonded carbon arises from C^+ ions penetrating surface layers, and giving a quenched-in density increase. Some results[11] indicate that three factors are responsible for the highly tetrahedral nature of the resulting DLC films, (i) a nearly fully ionized plasma beam, (ii) the presence of one dominant ion species and (iii) the mono-energetic character of the beam. In our previous study,[12] we proposed the deposition processes of DLC films, where the film properties are mainly associated with surface diffusion and growth induced by low-energy particles, and deep-layer implantation of high-energy ions. The properties of DLC films may change from those of polymer-like to diamond-like to graphite-like, depending on the incident particles and energy distribution.

In this paper, we prepare DLC films by filtered pulsed cathodic arc discharge (PCAD), ECR-plasma source ion implantation (PSII) and low-pressure DBD plasma. The effects of some discharge parameters on film properties are studied. Based on the experimental results, the DLC film deposition processes are analysed.

*Project supported by National Natural Science Foundation of China (Grant No 10405005).
†E-mail: Dongping.liu@dlnu.edu.cn

2. Experimental procedure

Hydrogenated DLC films on silicon substrates were obtained from low-pressure DBD plasma and ECR-CVD. The details of the low-pressure DBD plasma deposition system at 1.4kHz power frequency were described elsewhere.[9] The films were deposited in CH_4/He plasmas at gas spacing of 8mm under the total discharge pressure of 150Pa. The ECR-PSII apparatus consisted of two microwave ECR plasma sources located opposite to each other at the two sides of one vacuum chamber, and one pulse negative high voltage source. A –20 kV pulsed voltage was applied to the substrate holder to accelerate ions in the plasma. The ion implantation process was produced at the pulse width of 20μs with a pulse frequency of 100Hz. The DLC films were grown in methane–hydrogen or acetylene–hydrogen plasmas with a total gas pressure of 0.1Pa. To analyse the film deposition processes, we also prepared the films by using the ECR plasma sources while the negative high voltage source was switched off. The filtered-PCAD method was used to prepare ta-C films on silicon substrates.[13] The deposition was performed at the following discharge parameters: pulse duration 300μs, pulse repetition time 0.5s, and cathode–anode discharge voltage 200–400V.

Nanoindentation experiments were performed using an atomic force microscope (AFM system, DI Dimension 3100) and a diamond-tipped cantilever. A pyramidal diamond tip with the tip radius smaller than 25 nm was used to generate the indentation impressions. The applied loading force was deduced from the bending of the actual cantilever and its spring constant. The nanohardness was defined as the ratio of the indentation force to the projected area of the residual indentation.[14,15] The nanoindentation tests show the silicon (100) has the hardness of 11GPa $\pm$ 15% at the indentation force ranging from 40 to 100μN. The wear tests were conducted at a given loading force for an increasing number of wear cycles and the thickness of soft layers at film surfaces was estimated from the curves of the wear depths versus the number of wear cycles.[12–16]

The conducting-AFM (C-AFM) tests were performed at the regions of the wear marks. The experimental setup for C-AFM has been previously described in detail.[16] Briefly, a constant voltage was applied between the conducting tip and the substrate, and Fowler–Nordheim (F–N) currents were measured simultaneously with topography.

3. Results and discussion

The deposition conditions and corresponding film characteristics, such as surface layer thickness, RMS roughness, estimated nanohardness, and deposition rates are listed in Table 1. The ta-C films with the nanohardness of 50–60GPa were deposited using filtered PCAD. The root-mean-square (rms) roughness and hardness of ta-C films remained nearly constant with increasing cathode–anode voltage. The ta-C films were covered with thin (0.7–0.9 nm) surface layers. The deposition rates increase with increasing cathode–anode voltage due to the higher stored energy of main discharge capacitor at higher cathode–anode voltage. The formation of soft surface layers can be associated with the density of low-energy particles.[16] The low-energy particles have insufficient energy to change the atomic arrangements at the film surface, and they form the graphite-like structure at the film surface.

The surface layer thickness of DLC films obtained from ECR-PSII decreases from 4.0 to 1.5 nm with H/C ratio of reactive gases increasing from 4.0 to 9.1, which is well associated with the variation of deposition rates with H/C ratio. The surface layer structure of ta-C and hydrogenated DLC films can be seen from C-AFM measurements (Fig.1). The wear depths of ta-C and hydrogenated DLC films are 0.9 and 2.5 nm, respectively. The emission current images (Fig.1(b) and 1(d)) of the wear marks are obviously consistent with their topographic images (Fig.1(a) and 1(c)). Compared with the region where the soft surface layer exists, the wear mark at the surface of the ta-C film is more insulating (Fig.1(a) and 1(b)), which indicates that the surface layer of ta-C films has graphite-like structure.[16] The wear mark at the surfaces of the hydrogenated DLC film is more conductive, compared with the region where the 2.0 nm soft surface layer exists. This soft surface layer of hydrogenated DLC films obviously leads to a reduction of the nanotip emission area. The results show that the surface layer of hydrogenated DLC films is more insulating compared with the bulk structure, and shows a surface structure rich in hydrogen and sp^3 hybridized carbon, as measured by surface-sensitive EELS.[17]

Table 1. DLC deposition conditions and film characteristics.

DLC deposition method	discharge voltage/V	H/C ratios of reactive gases	He/CH_4 ratios of reactive gases	thickness of surface layers	RMS roughness/nm	nanohardness /GPa	deposition rate/(nm/min)
Filtered-PCA	200			0.8	0.13	50	1.2
Filtered-PCA	250			0.7	0.15	48	1.4
Filtered-PCA	300			0.9	0.13	55	1.7
Filtered-PCA	350			0.8	0.14	58	2.0
Filtered-PCA	400			0.8	0.14	56	2.4
ECR-PSII		1.00			3.96		
ECR-PSII		1.74			4.72		
ECR-PSII		3.00			5.10		
ECR-PSII		4.00		4.0	0.27	18	1.37
ECR-PSII		4.94		3.2	0.40	17	1.07
ECR-PSII		6.14		2.3	0.25	16	0.81
ECR-PSII		7.82		2.0	0.20	17	0.64
ECR-PSII		8.08		1.7	0.25	18	0.60
ECR-PSII		9.14		1.5	0.21	13	0.55
ECR		8.08			0.39	2.3	2.04
DBD			0.0		0.50	2.0	3.1
DBD			0.1		0.35	2.7	2.9
DBD			0.2	2.4	0.28	7.4	2.6
DBD			0.3	2.2	0.26	9.4	2.3
DBD			0.5	1.85	0.22	17.4	1.1
DBD			0.6	1.8	0.20	17	0.8

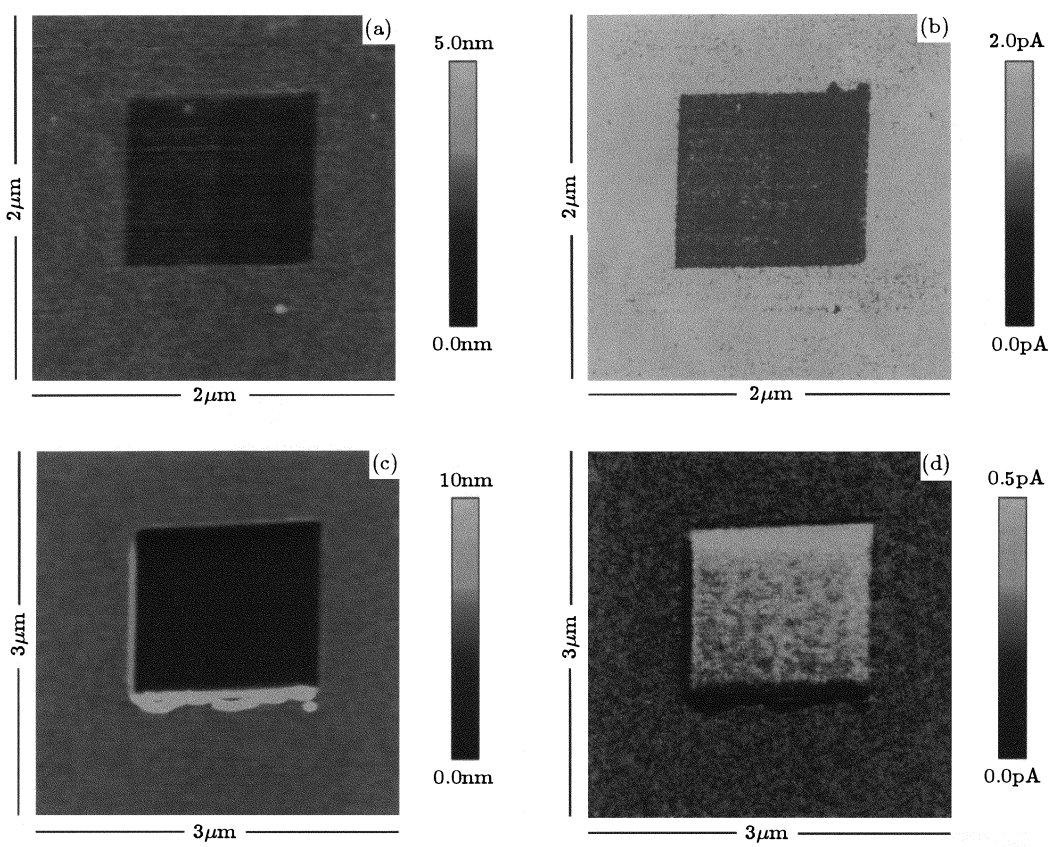


Fig.1. Topographic drawing ((a) and (c)) and simultaneously measured current image ((b) and (d)) for the regions of wear marks produced on the 120 nm ta-C film from filtered-PCAD ((a) and (b)) and the 80 nm hydrogenated DLC film from ECR-PSII ((c) and (d)). Their surface layer thickness and wear depths are ((a) and (b)) 0.9 and 0.9 nm; ((c) and (d)) 2.0 and 2.5 nm, respectively.

Deposition from ECR-PSII at H/C ratio of reactive gases higher than 4.0 gives a hardness of 15–20GPa and surface rms roughness of 0.2–0.4 nm. The films deposited at lower H/C ratios, typically in the range of 0.3 to 1.0 exhibit a rms roughness of 4.0–8.5 nm. The plasma contains plenty of radicals and excited particles. The unusual high rms roughness of the films deposited at lower H/C ratios is presumably due to the rapid deposition of the low-energy particles generated by ECR plasma sources. The high-energy ions accelerated by the pulse negative bias could not efficiently eliminate the voids and rough particles formed by the high surface atomic mobility.[18] The film from ECR plasma sources exhibits a hardness of $\sim$ 2GPa, and has polymer-like structure, which was proven by infrared spectroscopy.

The ion temperature in the ECR plasma is typically lower than 0.6 eV and the ion density varies in the range of 0–20% depending on the discharge pressure and microwave power.[19,20] The implanted ions accelerated across the sheath have energies ranging from the plasma potential to the pulse voltage (20 kV). The implanted ions with the maximum energy up to 20 kV can penetrate 1.5–4.0 nm surface layers[21] and produce a strong thermal spike, as shown in Fig.2. At a H/C ratio of 8.08, the deposition rate of the film obtained with the ECR plasma sources is 3.5 times higher than the one with ECR–PSII. The thermal spike can cause the atomic rearrangement within the film, followed by the high sputtering rate because of the lower film deposition rates with ECR-PSII. The low-energy particles generated by ECR plasma sources have insufficient energy to penetrate the film surface and form soft polymer-like structure at the surface. The atomic hydrogen in the ECR plasmas may lead to the transformation of sp^2 hybridized carbon group to sp^3 hybridized carbon group at the film surface, and contribute to the formation of hydrogen and sp^3 hybridized carbon enriched surface layers. If the film with ECR-PSII has one stable surface layer formed by low-energy particles, the average film deposition rate ($\bar{r}$) may be expressed as

$$\bar{r} = J_{\rm l} + \bar{J}_{\rm i} = \bar{J}_{\rm t}, \qquad (1)$$

where $J_{\rm l}$ is the deposition flux due to the low-energy particles that are not subsequently sputtered from the surface, $\bar{J}_{\rm i}$ is the average sputtering rate due to the high-energy ion implantation, and $\bar{J}_{\rm t}$ the net atomic amount transferred from the surface layer to the bulk phase due to the ion implantation. The sputtering due to the high-energy ion bombardment removes the surface atoms, whereas the implanted atoms from the surface layer cause a net growth of the film. The implantation process also causes the release of hydrogen from the bulk phase, and leads to an increase in film density.

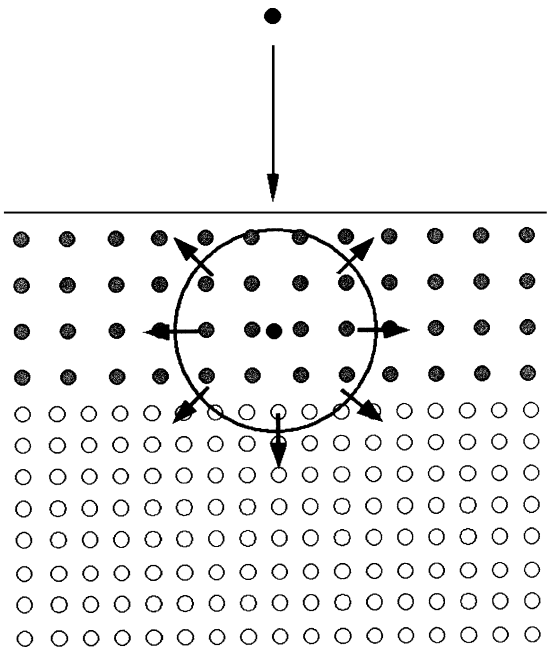


Fig.2. A thermal spike produced by high-energy ion bombardment. The film is covered with a soft surface layer. The intense local heating from the thermal spike can provide the energy required to release atoms from their metastable positions in a spheroidal volume.

Both deposition rates and surface layer thickness of hydrogenated DLC films from DBD plasmas decrease with increasing He/CH_4 ratio of reactive gases. The formation of soft surface layers can be associated with the density of the low-energy CH_x groups generated in DBD plasmas. The higher He/CH_4 ratios contribute to the formation of DLC films with thinner surface layers because of the lower density of CH_x groups. The film hardness increases from 2 to 17 GPa with increasing He/CH_4 ratio, indicating that the film properties change from those of polymer-like to diamond-like. The films with higher hardness exhibit thinner surface layers. Some higher-energy particles may produce stronger thermal spikes within the soft surface layer (Fig.2). The thermal spikes can cause the atomic re-arrangement beneath the surface layer and lead to an increase in film density. The formation of thinner surface layers indicates that more high-energy ions penetrate the surface layer, which contributes to an improvement of film hardness. RMS roughness decreases from 0.5 to 0.2–0.3 nm with increasing He/CH_4

ratio. The surface growth induced by low-energy CH_x groups can cause an increase in surface roughness. The ion implantation processes may contribute to the formation of DLC films with smoother surfaces.[10] At higher He/CH_4 ratios, the film growth can be governed by the energetic ion implantation because of lower density of CH_x groups.

The ions from cathodic arc discharge have the most probable energy at about 20 eV and are primarily (>95%) in the first ionization state.[22] These ions have insufficient energy to penetrate film surface. However, they may produce one energetic impact at the film surface and form a thermal spike. The intense local heating from the thermal spike can provide the energy required to release atoms from their metastable positions. The ta-C films can be obtained when the intense local heating can be efficiently dissipated to the sp^3 bonded lattice.[23] Our recent experimental results also indicate that the sp^3 bonding can be efficiently formed at an sp^3 bonded matrix, compared with the sp^2 sites. The ion energy from a thermal spike may be transferred to the atoms beneath the thinner (2–3 atomic distances) graphite-like surface layers,[24] and leads to the formation of an sp^3 bonded structure at an sp^3 bonded matrix.

4. Conclusion

Surface properties of hydrogenated DLC and ta-C films have been analysed using AFM-based tests. Experimental results show that soft surface layers of ta-C films have graphite-like structure while hydrogenated DLC films have H and sp^3 enriched surface layers. For typical CVD methods, film growth is governed by low-energy particles. The surface diffusion and growth induced by the low-energy deposition process lead to the formation of polymer-like soft surface layers. The thickness of soft surface layers, typically in the range of 1.5–4.0 nm is related to film deposition rate. High-energy ion implantation can cause the release of hydrogen from solid-state structure, and lead to an increase in film density. The ta-C films can be produced in highly ionized plasmas by the deposition from medium energy carbon ions. Some low-energy particles have insufficient energy to cause atomic re-arrangements at film surface, and thus form the graphite-like structure.

References

[1] Kudoyarova V, Chernyshov A, Zvonareva T, Dzhelepova N and Tsolov M 1998 *Surf. Coat. Technol.* **100–101** 192

[2] Polo M, Andujar J, Hart A, Robertson J and Milne W 2000 *Diamond Relat. Mater.* **9** 663

[3] Cuomo J, Pappas D, Bruley J and Doyle J 1991 *J. Appl. Phys.* **70** 1706

[4] Miyagawa S, Nakao S, Saitoh K, Baba K and Miyagawa Y 2000 *Surf. Coat. Technol.* **128–129** 260

[5] Martinez E, Polo M, Pascual E and Esteve J 1999 *Diamond Relat.* Mater. **8** 263

[6] Xu J, Huang X, Li W, Wang L and Chen K 2002 *Chin. Phys.* **11** 502

[7] Yang W, Wang J, Zhang G, Fan S, Liu C and Yang S 2003 *Chin. Phys.* **12** 1257

[8] Rusli A, Yoon S, Yang H, Zhang Q, Ahn J and Fu Y 1998 *J. Vac. Sci. Technol.* A **16** 572

[9] Liu D, Ma T, Yu S, Xu Y and Yang X 2001 *J. Phys.* D *Appl. Phys.* **34** 1651

[10] Robertson J 1994 *Pure Appl. Chem.* **66** 1789

[11] Weiler M, Robertson J, Sattel S, Veerasamy V, Jung K and Ehrhardt H 1995 *Diamond Relat. Mater.* **4** 268

[12] Liu D, Benstetter G, Lodermeier E, Akula I, Dudarchyk I, Liu Y and Ma T 2003 *Surf. Coat. Technol.* **172** 194

[13] Stanishevsky A 1999 *Chaos Solitons & Fractals* **10** 2045

[14] Jiang Z, Lu C, Bogy D, Bhatia C and Miyamoto T 1995 *Thin Solid Films* **258** 75

[15] Prabhakaran V and Talke F 2000 *Wear* **243** 18

[16] Liu D, Benstetter G and Frammelsberger W 2003 *Appl. Phys. Lett.* **82** 3898

[17] De Martino C, Demichelis F, Tagliaferro A, Patrini M, Rizzi A, Fontaine M and Layet J 1995 *Diamond Relat. Mater.* **4** 996

[18] Fung M, Chan W, Lai K and Bello I 1999 *J. Non-Cryst. Solids* **254** 167

[19] Shindo M, Hiejima S, Ueda Y and Kawakami S 1999 *Thin Solid Films* **345** 130

[20] Koga M, Yonesu A and Kawai Y 2003 *Surf. Coat. Technol.* **171** 216

[21] Nelson R, Hudson J, Mazey D and Piller R 1983 *Proc. R. Soc. Lond* A **386** 211

[22] Lossy R, Pappas D, Roy R, Doyle J and Bruley J 1995 *J. Appl. Phys.* **77** 4750

[23] Lee S, Lee C, Lee S and Lee K 2004 *Surf. Coat. Technol.* **177–178** 812

[24] Seitz F and Turnbull D 1956 *Solid State Phys.* **2** 305